Digest Journal of Nanomaterials and Biostructures Vol. 10, No. 3, July - September 2015, p. 837 - 845

AN INVESTIGATION OF THE EFFECTS OF CONVENTIONAL AND MICROWAVE HEATING SYSTEM ON THE DOPING OF GRAPHENE OXIDE WITH Ni IN AQUEOUS SOLUTION

R. M. K. VALA[a], C. W. DIKIO[a], N. AYAWEI[b], F. M. MTUNZI[a],
E.D. DIKIO[a*]
[a]Applied Chemistry and Nanoscience Laboratory, Department of Chemistry, Vaal University of Technology, P. O. Box X021, Vanderbijlpark 1900, Republic of South Africa
[b]Department of Chemical Sciences, Niger Delta University, Wilberforce Island, Bayelsa State, Nigeria

Graphene oxide (GO) have been synthesized and doped with nickel metal salt under differ thermal conditions. The doped graphene oxides obtained were characterized by Fourier transform infrared spectroscopy (FTIR), Scanning electron microscopy (SEM), Transmission electron microscopy (TEM), Raman spectroscopy, and Atomic force spectroscopy AFM). The results obtained indicate difference between the crystallinity pattern of microwave and the conventional heating system of the materials and the progressive formation of transparent and decorated graphene with nickel particles which increases with temperature.

(Received May 12, 2015; Accepted July 27, 2015)

Keywords: Graphene, Nickel doped, AFM, Transparent

1. Introduction

Graphite is one of the most well-known forms of elemental carbon found in nature. It is used to prepare graphene which is attracting enormous interest in the research community because of its potential applications [1,2]. Thus, various methods have been used to tailor the graphene properties for desired applications. Chemical doping, electrochemical doping, and metal contact doping are some of the most interesting methods used to tailor the graphene properties. Potassium, boron, and nitrogen are some of elements used for doping graphene. Consequently, a shift in the properties of the host material, such as the chemical potential has been reported in the literature [3-8]. Also, the doping of graphene has shown modulated effect on the fundamental electron-phonon interactions properties of graphene, such as the breakdown of the adiabatic Born-Oppenheimer approximation, the interplay between adiabatic and non-adiabatic effects or the interference between all the quantum pathways involved in inelastic light scattering [9-13].

Nickel has ferromagnetism property [14] around room temperature. Therefore, the use of nickel for doping graphene is expected to improve the above fundamental properties. Dahal and Batzill [15] reported that the ferromagnetic nickel induces a magnetic moment in the carbon. Furthermore, the authors stated that as substrate in chemical vapour deposition (CVD), nickel induced geometric and electronic changes and altered the phonon dispersion which caused the monolayer graphene on nickel not to exhibit a Raman spectrum. Others such as Wei et al. [16] doped graphene/carbon cryogels with nickel and investigated the adsorption properties of the prepared materials for the removal of dyestuffs from water purification [17] produced $Ni(OH)_2$ nanocrystals on graphene sheets to explore its electrochemical pseudo capacitor properties as potential energy storage material. When investigating the electronic, structural and transport properties of Ni-doped graphene, [18] found that the Ni (lying along the edge of zigzag graphene

---

[*] Corresponding author: ezekield@vut.ac.za

nanoribbons) exhibited an energetic preference for the hole sites within the graphene lattice. In their review on graphene-nickel interfaces, [15] explained that this interaction is due to hybridization of the metal d-electrons with the π-orbitals of graphene.

When microwave is used as source of energy, matter absorbs the radiation and the process is known as dielectric heating [19]. It has been reported [20] that microwave heating (a non-conventional energy source), applied in numerous fields, leads to dramatically reduce reaction times, increased product yields and enhanced product purities by reducing unwanted side reactions compared to the conventional method of heating.

Although Ni-doped graphene has been documented, no report was found on the effects of conventional and microwave on the doping of graphene with nickel, using atomic force microscopy (AFM) and the Raman spectroscopy as characterization techniques. Therefore, in this work, we report a single and one step method for preparing Ni-doped graphene by directly using GO sheets and its characterization by AFM and Raman spectroscopy, supported by FT-IR, TGA, SEM, and XRD.

2. Materials and Methods

2.1 Materials

Graphite was obtained from Sigma-Aldrich, Hydrogen peroxide from Labchem, Hydrochloric acid from associated chemical enterprises (ACE), $NiCl_2.6H_2O$ (98%) and H_2SO_4 from Merck, and $KMnO_4$ from Univar.

2.2. GO synthesis

GO was prepared by oxidation of graphite according to the modified method from [21]. 92 mL concentrated H_2SO_4 were mixed with 12 g $KMnO_4$ in a 1000 mL beaker and stir at 0°C for 30 min. After that, 4 g of graphite flakes were added and the mixture was stirred for 72 h. Distilled water (184 mL) was added slowly into the paste and the temperature was maintained below100°C. After 15 min 20 mL of 30% H_2O_2 solution were added and shaken for 10 min. The mixture was filtered with 500 mL 10% HCl to remove metal ions. Finally, the mixture was thoroughly washed with distilled water and oven dried overnight at 35°C.

2.3 Ni doped GO

200 mg GO were ultrasonicated in 15 mL of water for 30 min to allow exfoliation and then 50 mL of 0.04M of $NiCl_2.6H_20$ were added. The mixture was shaken for 3 h under the following conditions: room temperature (rt), 50, 70, and 90°C (conventional heating) in a water bath; and 10 min in a household microwave.

3. Results and discussion

Graphene oxide and doped graphene oxide using nickel salt obtained in this synthesis were black/dark flaky material. The resulting materials were investigated by means of FT-IR, TGA, SEM, XRD, AFM, and Raman spectroscopy. Metal-π interactions which involve interaction of nickel and the π system of graphene are assumed to be the driving force to sustain the doping of nickel.

3.1 FT-IR results

Fourier transform infrared spectroscopy (FT-IR) spectra were recorded with a PerkinElmer FT-IR/FT-NIR spectrometer; results are presented in Figures 1 (a and b) for the conventional heating system. The broad band around 3293 cm^{-1} is due to the vibration of hydroxyl OH group. The peak at 1733 cm^{-1} due to C=O, the peak at 1616 cm^{-1}assigned to the C=C bond, the peak at 1368 and 1228 cm^{-1} to the C-H bond, and 1055 $cm^{-1}$to C-O-C bond. The small peak (shoulder) at 836 cm^{-1} was attributed to the vibration of O-Ni bond [22,23]. Not much differences were observed with the increasing temperature (at 90°C) (Figure 1b) except some small shift of peaks; also, the peak at 843 and 703 cm^{-1} (assigned to C-Cl bond) became more evident, whereas the peak at 972 cm^{-1} was less noticeable.

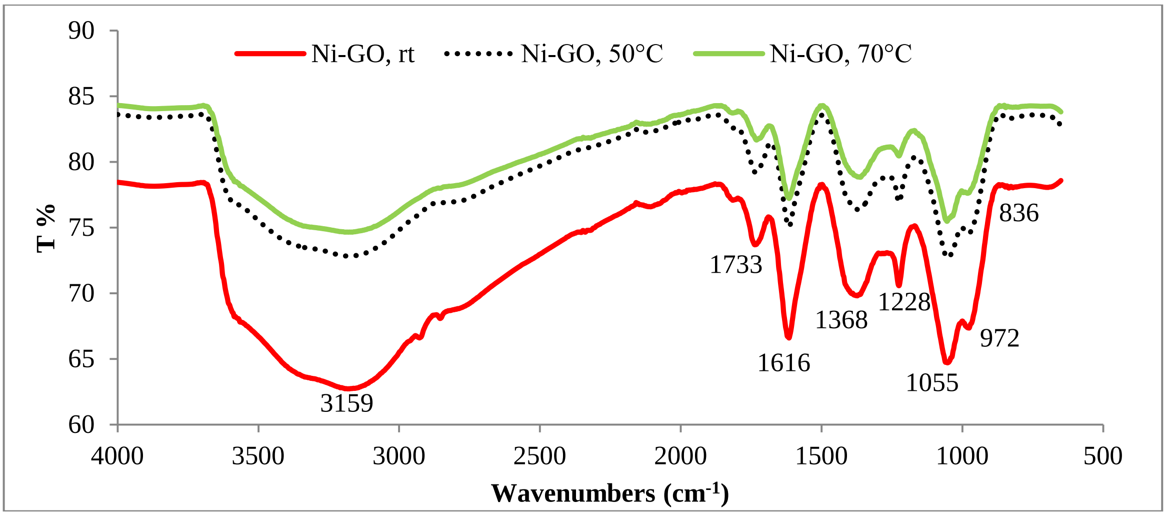

Fig. 1a: FT-IR of Ni-doped graphene at different temperature

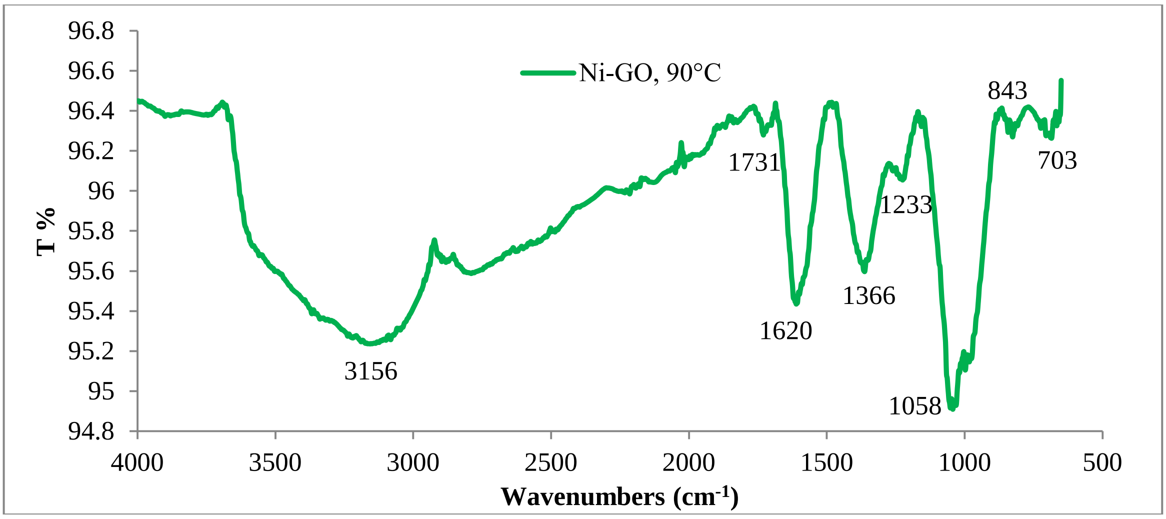

Fig. 1b: FT-IR of Ni-doped graphene at 90°C

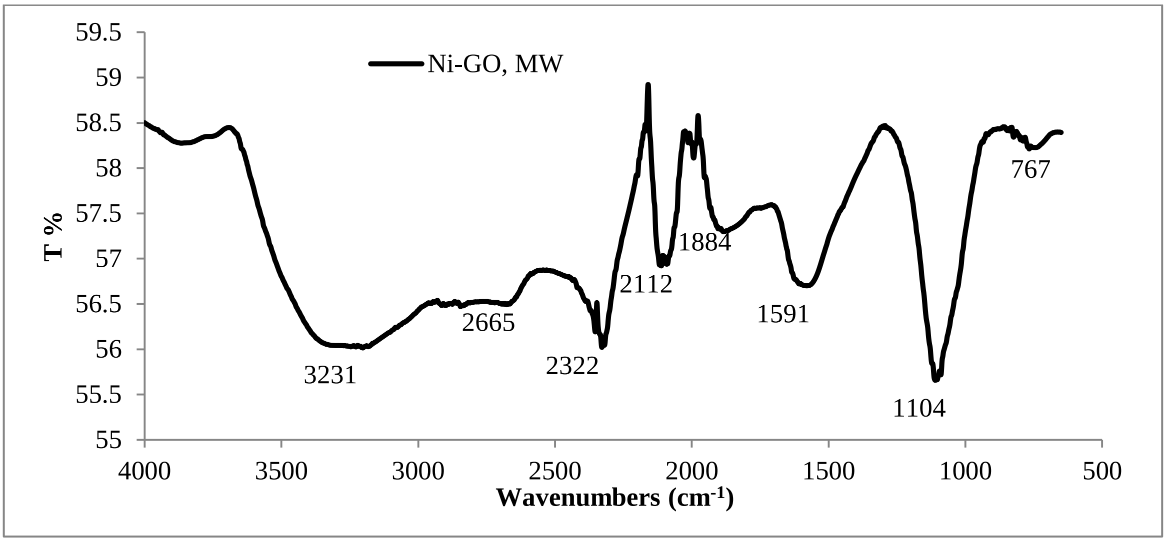

Fig. 1c: FT-IR of Ni-doped graphene using microwave irradiation

When the nickel doped graphene was heated in a microwave oven and analysed (Figure 1c), we observed the appearance and disappearance of vibration bands, indicating different effects of this source of energy on the doping. Peaks at 686, 827, 1226, 1366 cm^{-1} disappeared; peak at 1730 cm^{-1} was reduced to a small shoulder while peak at 1043 cm^{-1} and 1605 shifted. New peaks appeared at 767 cm^{-1}, 1884, 2112, 2322, and a small one at 2665 cm^{-1}. The peak at 767 cm^{-1} was assigned to the C–Cl bond, the peak around 1104 cm^{-1} assigned to the C–O bond, and the peak around 1591 cm^{-1} to the C=C bond. The peak at 1884 cm^{-1} was attributed to the formation of an acid anhydride, the peak at 2112 cm^{-1} attributed to the terminal C≡C, the peak at 2322 cm^{-1} to the methoxy group (CH_3–O–R), and the peak around 3275 cm^{-1} was assigned to the alkyne C–H and O-H. It has been reported [24-25] that the effect of microwave irradiation in organic synthesis is a combination of thermal effects, arising from the heating rate, superheating or ‘‘hot spots’’ and the selective absorption of radiation by polar substances. Therefore, it is likely that the new vibration bands could result from the combination of the microwave thermal effects and the presence of Ni which probably played a double role as dopant and catalyst (for deprotonating the double bond, C=C, lying along the edge of zigzag graphene). We assumed; however, that the microwave could have produced different effects on the materials, such as splitting the water and graphene into radicals, promoting the breaking down and formation of bonds which are observed in the FT-IR spectra.

3.2 Morphology

Results of Ni-doped graphene were examined with TEM (Figure 2) to explain the structure of the obtained products. Micrographs show more heterogeneous structure with increased temperature. Figure 3(a-e) illustrates the micrographs of Ni-doped graphene at different temperature conditions. These micrographs exhibit a transparent structure of graphene decorated with Ni particles. The decoration increases with temperature, especially when the doping was conducted under microwaves conditions, as illustrates in Figure 3(e). SEM images are correlated to TEM results, suggesting specific effect of temperature on the doping of graphene with nickel salt. Similar results were obtained by [26,27].

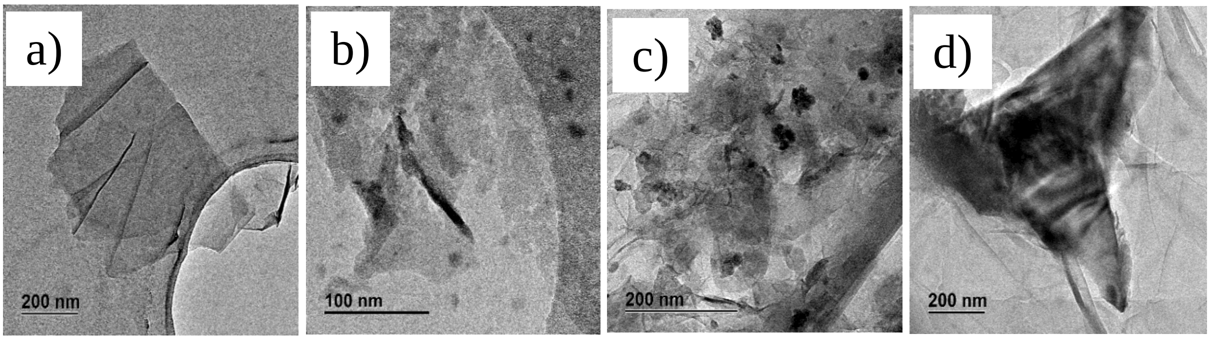

Fig. 2: Transmission Electron Microscope (TEM) images of Ni-doped GO:
a) @ rt, b) @ 50°C, c) @ 70°C, d) @ 90°C

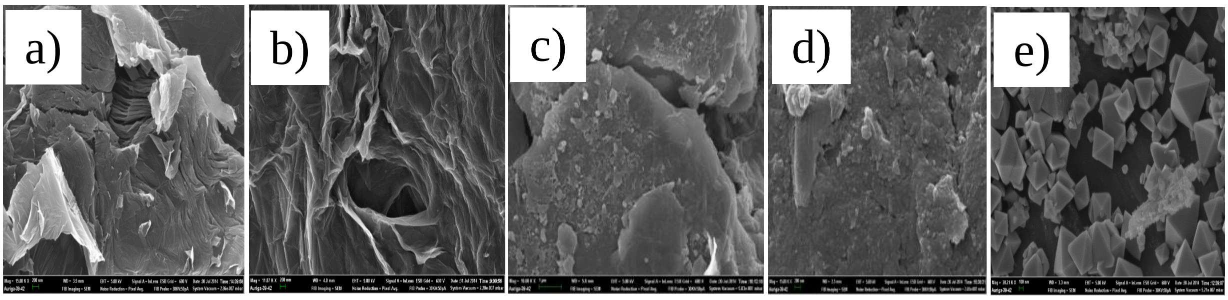

Fig. 3: SEM images of Ni-doped graphene: a) @ rt, b) @ 50°C, c) @ 70°C, d) 90°C, and in Microwave

3.3 XRD results

XRD was used to characterize the Ni-doped samples. The XRD patterns of Ni-doped graphene are presented in Figure 4. Beside the common peaks observed when the conventional heating system was used, microwave Ni-doped graphene spectrum presents new peaks which are observed at $2\theta = 36.8, 42, 62.5, 75, 79°$ and the broad peak around $2\theta = 25°$. The appearance of new peaks highlights the dielectric heating effects of microwave as reported [20] and shows that microwave increases the crystalline structure of the doped graphene.

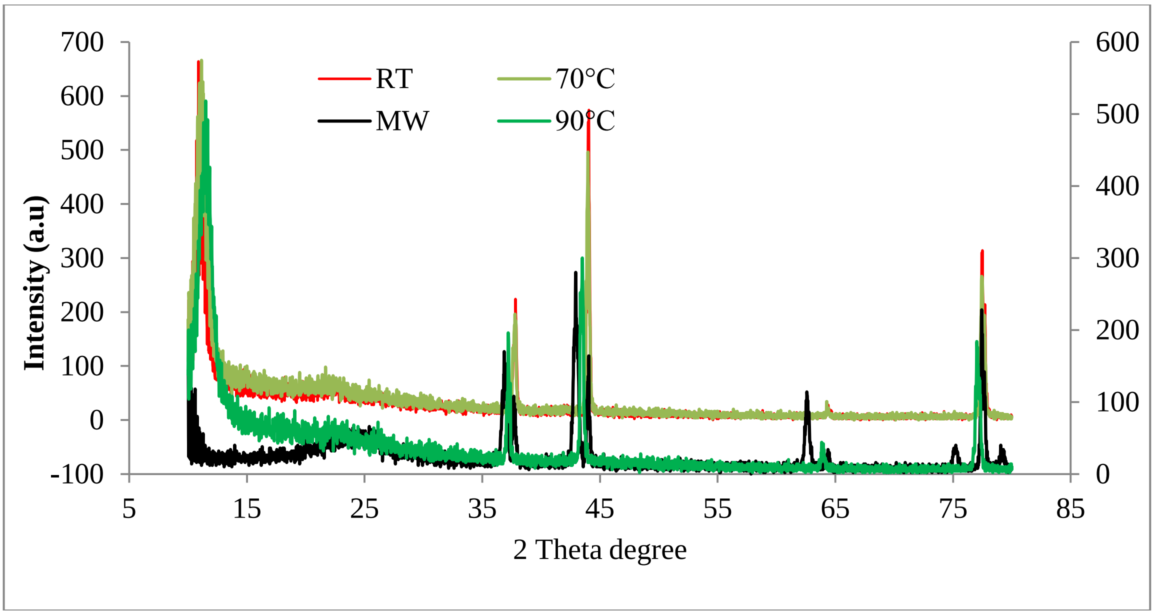

Fig. 4: XRD results of Ni-doped graphene

3.4 AFM results

Atomic Force Microscopy (AFM) is one of the most important widely used tools for imaging, measuring and manipulating matter at the nanoscale. It is not only used to image the topography of surfaces, but can serve to measure other parameters, such as electric and magnetic properties, and chemical potentials. Therefore, analysis of nickel doped graphene was carried out to identify layers of graphene flakes and to study flakes shape, uniformity, and other properties. AFM was used to characterize the doped graphene oxide with nickel conducted under normal heat (from room temperature, ~25°C, to 90°C) and microwave. The general feature of the AFM height images (Fig. 5(a-f) showed that with increasing temperature, the surface coverage gradually changed from a typical flatten exfoliated nanosheets-like to homogeneity with reduction of “ripples”, through brighter loops/globular, “peapod-like graphic”, scratches, and wrinkles. Such observation has been reported by other researchers [28,29]. Whereas, the phase micrographs (not presented here) showed a landscape varying from a busy fibrous (due to suspension of Ni particles) to homogeneity through “seed spread-like” system, as the temperature increased. The ripples are likely to be originated from the doping with nickel. The above described micrographs changes suggested that: 1) Ni particles are well dispersed with increasing temperature and 2) the presence of new bond between Ni and C in the lattices of the graphene sheet, due to doping. Topographic images (Figures 5 a, b, c, d, and e); however, revealed multilayer systems with ripples and is not perfectly flat. When microwave was used as source of heat, the AFM topography of Ni doped graphene (Figure 6 f) reveals localised ripples of clusters of nickel (in polygonal shape) than the graphene sheet.

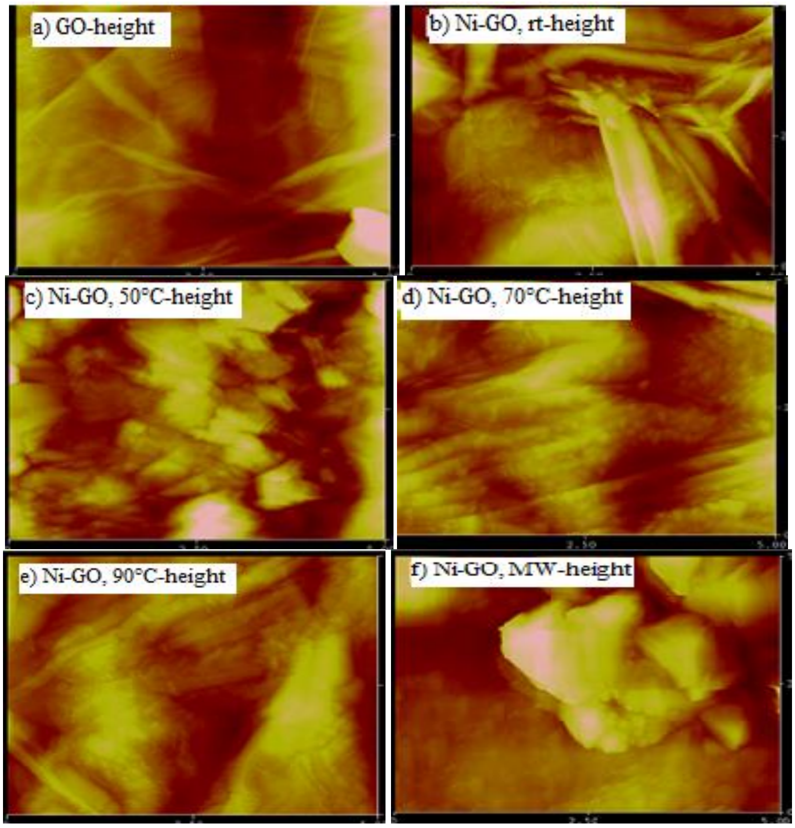

Fig. 5: Atomic Force Microscope (AFM) images of graphene

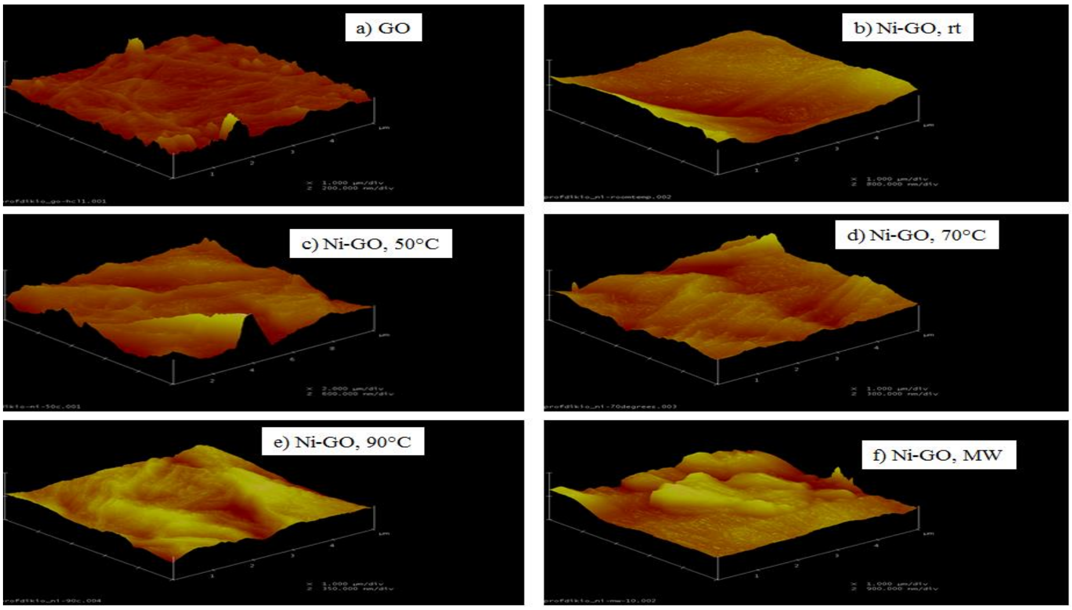

Fig. 6: Topographic images of GO and Ni doped GO at different temperatures.

3.5 Raman results

Raman spectroscopy is one of the most reliable research techniques for identifying and characterizing all the members of the carbon family, both at the lab- and at mass-production scale [30]. The Raman spectra of carbon systems few prominent features with intense bands in the 1000–2000 cm^{-1} region, giving enough information to distinguish different types of carbon, such as amorphous carbon and carbon nanotubes [31]. The most prominent phonon modes in two-dimensional carbon lattices are as follows: (i) the G band (highly sensitive to the number of layers and small amounts of strain present on the sample), which is centred around 1580 cm^{-1} in intrinsic graphene, (ii) the D (intensity directly proportional to the level of defects in the sample) mode around 1340 cm^{-1}, (iii) the 2D mode (around 2670 cm^{-1}), which is an overtone of the D mode, due to the two-phonon nature of this mode, and (iv) the D' band [32-33].

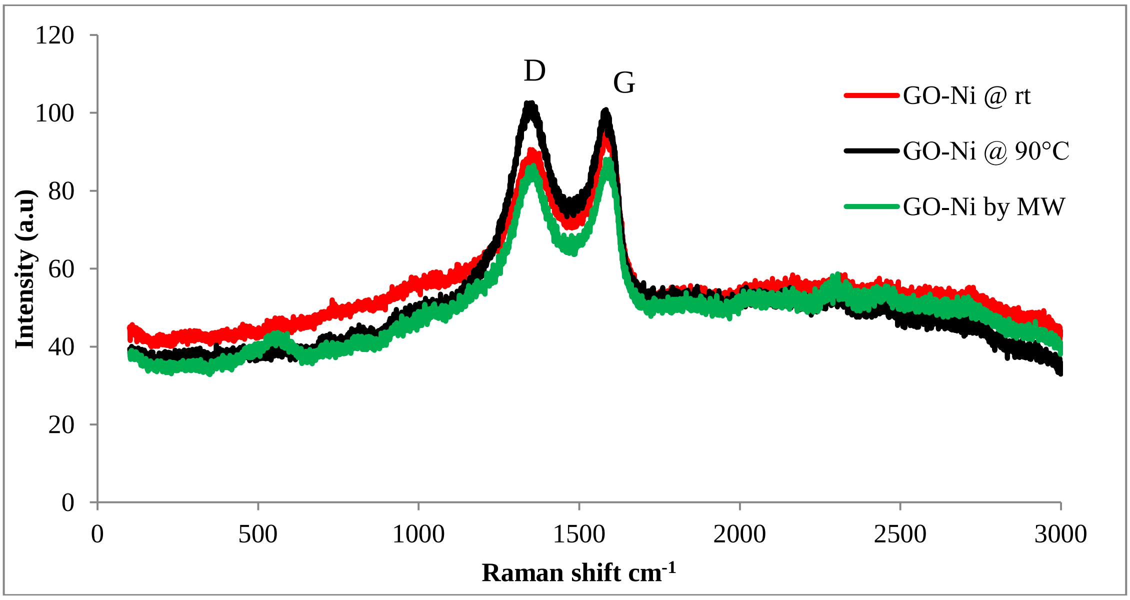

Fig. 7. Raman spectra of GO and Ni-doped graphene

Raman spectra of GO and Ni-doped graphene are compared, and Figure 7 shows a trend due to the effect of temperature, during the doping process, with only two peaks. As GO is exposed to Ni^{2+} ions at 90°C, the D peak, a signature for disorder at ~1338 cm^{-1}, induced by defects appear, displaying the increase of defects. The trend is reversed when doping is conducted at room temperature or under microwaves irradiation.

4. Conclusion

In this paper, graphene oxide was prepared and doped with nickel salt under conventional (from room temperature to 90°C) and microwave heat. Results showed a change in the crystallinityy of microwave Ni-doped compared to the conventional heating, the production of transparent sheets, and the increasing heat impacted the doping by decorating the nickel particles on the surface of graphene.

Acknowledgement

This work was supported by a research grant number (21542892/19032014) from the Research Directorate of the Vaal University of Technology Vanderbijlpark, South Africa.

References

[1] A.H.C. Neto, F. Guinea, N.M. R. Peres, K.S. Novoselov, A.K. Geim, Reviews of Modern Physics **81**, 109 (2009).
[2] A.K. Geim, K.S. Novoselov, The rise of graphene, Nature Materials, **6**, 183 (2007).
[3] L.S. Panchakarla, K.S. Subrahmanyam, S.K. Saha, A. Govindaraj, H.R. Krishnamurthy, U.V. Waghmare, C.N.R. Rao, Advanced Materials, **21**(46), 4726 (2009).
[4] D. Wei;, Y. Liu;, Y Wang., H. Zhang;, L. Huang;, G. Yu, Nano Lett., **9**(5), 1752 (2009).
[5] C. Zhang, L. Fu, N. Liu, , M. Liu, , Y. Wang, Z. Liu, Advanced Materials, **23**(8), 1020 (2011).
[6] L. Zhao, R. He, K.T. Rim, , T. Schiros, K.S. Kim, , H. Zhou, C. Gutiérrez; S. P. Chockalingam; C.J. Arguello;, L. Pálová;, D. Nordlund;, M.S. Hybertsen; D.R. Reichman; T.F. Heinz;, P. Kim;, A. Pinczuk, , G.W. Flynn, A.N. Pasupathy, Science, **333**(6045), 999 (2011).
[7] Z. Sun, Z. Yan; J. Yao, E. Beitler; Y. Zhu, J.M. Tour, Growth Nature **468**(7323), 549 (2010)
[8] T. Wu, H. Shen, L. Sun, , B. Cheng; B. Liu, J. Shen, New J. Chem., **36**(6), 1385 (2012).
[9] A. Tiberj, M. Rubio-Roy, M. Paillet, J.-R. Huntzinger;, P. Landois;, M. Mikolasek;, S. Contreras, J.-L. Sauvajol;, E. Dujardin; Zahab, A.-A. Scientific Reports, **3**(2355), 1 (2013).
[10] S. Pisana, M. Lazzeri;, C. Casiraghi;, K.S. Novoselov, A.K. Geim;, A.C. Ferrari;, F. Mauri, Nature Materials **6**, 198 (2007).
[11] A. Das, S. Pisana, B. Chakraborty, S. Piscanec, S. K. Saha;, U.V. Waghmare, K.S. Novoselov, H.R. Krishnamurthy, A.K. Geim, A.C. Ferrari, A.K. Nature Nanotechnology **3**, 210 (2008)
[12] C.-F. Chen, C.-H. Park;, B.W. Boudouris;, J. Horng;, B. Geng, C. Girit;, A. Zettl, M.F. Crommie;, R.A. Segalman;, S.G. Louie, F. Wang, Nature **471**, 617 (2011).
[13] R. Parret, M. Paillet, J.-R. Huntzinger, D. Nakabayashi, T. Michel; Tiberj, Antoine; Sauvajol, Jean-Louis; Zahab, Ahmed A. ACS Nano, **7**, 165 (2013).
[14] D.G.E Kerfoot, "Nickel", Ullmann's Encyclopedia of Industrial Chemistry, Weinheim: Wiley-VCH, 2005, DOI: 10.1002/14356007
[15] A. Dahal;, M. Batzill, Nanoscale **6**, 2548 (2014).
[16] G. Wei, Y.-E Miao, C. Zhang, Z. Yang, Z. Liu, , W.W. Tjiu, T. Liu,

ACS Applied Materials & Interfaces **5**, 7584 (2013).
[17] H. Wang, H.S. Casalongue, Y. Liang, H. Dai, J. Am. Chem. Soc. **132**, 7472 (2010)
[18] V.A. Rigo, T.B. Martins; A.J.R. Da-Silva, A. Fazzio, R.H. Miwa, Physical Review B, **79**, 075435 (2009).
[19] Antonio de la Hoz, Ángel Díaz-Ortiz and Andrés Moreno, Chem. Soc. Rev. **34**, 164 (2005).
[20] Borivoj Adnadjevic and Jelena Jovanovic (year) The Effect of Microwave Heating on the Isothermal Kinetics of Chemicals Reaction and Physicochemical Processes. In Stanisław Grundas (Ed.), Advances in Induction and Microwave Heating of Mineral and Organic Materials, (pp 391-422), In Tech Publisher. 2011
[21] W.S. Hummers, R.E. Offeman, Journal of the American Chemical Society **80**(6), 1339 (1958).
[22] J. Coates, Interpretation of Infrared Spectra, A Practical Approach. In R.A. Meyers (Ed.), Encyclopedia of Analytical Chemistry, (pp. 10815–10837), John Wiley & Sons Ltd, Chichester. 2000
[23] T. Mălăeru, J. Neamţu, C. Morari, G. Sbarcea, Revue Roumaine de Chimie **57**(9-10), 857 (2012).
[24] P. Lidström, J. Tierney, B. Wathey, J. Westman, Tetrahedron, **57**, 9225 (2001).
[25] A. De la Hoz, Á. Díaz-Ortiz, A. Moreno, Chem. Soc. Rev. **34**, 164 (2005).
[26] B. Adnadjevic, J. Jovanovic, The effect of microwave heating on the isothermal kinetics of chemicals reaction and physicochemical processes, In Stanislaw Grundas (Ed), Advances in Induction and Microwave Heating of Mineral and Organic Materials, 2011, (pp. 391-422), In Tech, Rijeka, Croatia
[27] X. Zhang, B. Jiang, Y. Xie, F. Du, Indian Journal of Chemistry **53A**, 265 (2014).
[28] M. Khenfouch, U. Buttner, M. Baïtoul, M. Maaza, Graphene, **3**, 7 (2014).
[29] R. Lv, Q. Li, A.R. Botello-Méndez, T. Hayashi, B. Wang, A. Berkdemir, Q. Hao, A.L. Elías, R. Cruz-Silva, H.R. Gutiérrez, Y.A. Kim, H. Muramatsu, J. Zhu, M. Endo, H. Terrones, J.C. Charlier, M. Pan, M. Terrones, Scientific Reports, , **2**(586), 2 (2012).
[30] K. Wang, Laser Based Fabrication of Graphene, In Mahmood Aliofkhazraei (Ed.), Advances in Graphene Science2013, (pp. 77-95), InTech.
[31] A.C Ferrari, Raman spectroscopy of graphene and graphite: Disorder, electron–phonon coupling, doping and nonadiabatic effects, Solid State Communications, **143**, 47 (2007).
[32] A.C. Ferrari, J. Robertson, Physical Review B, **61**(20), 14095 (2000).
[33] S. Heydrich, M. Hirmer, C. Preis, T. Korn, J. Eroms, D. Weiss, C. Schüller, Applied Physics Letters **97**, 043113 (2010).
[34] Y. Guo, X. Sun, Y. Liu, W. Wang, H. Qiu, J. Gao, Carbon, **50**(7), 2513 (2012).
[35] G. Sobon, J. Sotor, J. Jagiello, R. Kozinski, M. Zdrojek, M. Holdynski, P. Paletko, J. Boguslawski, L. Lipinska, K.M. Abramski, Optics Express, **20**(17), 19463 (2012).